Marine Pollution Bulletin 66 (2013) 151–157

Contents lists available at SciVerse ScienceDirect

Marine Pollution Bulletin

journal homepage: www.elsevier.com/locate/marpolbul

Physical dynamics controlling variability in nearshore fecal pollution: Fecal indicator bacteria as passive particles

M.A. Rippy [a,*], P.J.S. Franks [a], F. Feddersen [a], R.T. Guza [a], D.F. Moore [b,1]

[a] Scripps Institution of Oceanography, La Jolla, CA 92093-0218, USA
[b] Orange County Public Health Laboratory, Santa Ana, CA 92706, USA

ARTICLE INFO

Keywords:
Fecal indicator bacteria
Advection
Diffusion
Surfzone

ABSTRACT

We present results from a 5-h field program (HB06) that took place at California's Huntington State Beach. We assessed the importance of physical dynamics in controlling fecal indicator bacteria (FIB) concentrations during HB06 using an individual based model including alongshore advection and cross-shore variable horizontal diffusion. The model was parameterized with physical (waves and currents) and bacterial (*Escherichia coli* and *Enterococcus*) observations made during HB06. The model captured surfzone FIB dynamics well (average surfzone model skill: 0.84 {*E. coli*} and 0.52 {*Enterococcus*}), but fell short of capturing offshore FIB dynamics. Our analyses support the hypothesis that surfzone FIB variability during HB06 was a consequence of southward advection and diffusion of a patch of FIB originating north of the study area. Offshore FIB may have originated from a different, southern, source. Mortality may account for some of the offshore variability not explained by the physical model.

1. Introduction

Approximately 90% of California's beach closures are due to elevated levels of fecal indicator bacteria (FIB) (Dufour and Wymer, 2006). FIB are nonpathogenic enteric bacteria, present at high concentrations in human and animal wastes, that are used to track bacterial pathogens in coastal systems (Sinton et al., 1993). FIB are released from contaminated sources – often non-point source run-off or riverine discharge – become suspended in the surfzone (coastal waters shoreward of the breaker line), and are transported to beaches (Boehm et al., 2002, 2005; Grant et al., 2005). The spatial and temporal distribution of FIB sources, and the dynamics of the surfzone through which FIB are transported, play an important role in regulating the extent and intensity of beach bacterial contamination. Furthermore, because FIB survival in the surfzone determines the duration of transport, factors regulating FIB growth and mortality in coastal waters are also central to our understanding of bacterial pollution (Anderson et al., 2005; Boehm, 2003; Boehm et al., 2005).

Beach pollution events are often poorly predicted, and about 40% of contamination postings are erroneous (Kim and Grant, 2004). With over 550 million annual person-visits to California beaches, this inaccuracy impacts both individual beach goers and California's multi-billion dollar coastal tourism industry (Grant et al., 2001). Predictive modeling of bacterial pollution using readily measured (or modeled) physical parameters (wave height/direction, river flow, rainfall, etc.) could be a cost-effective way to improve the accuracy of beach contamination postings. However, to be effective in a range of settings, these models require mechanistic understanding of bacterial sources, transports, and extra-enteric growth or decay. Mechanistic understanding moves beyond correlations, and examines the effects of individual processes structuring beach pollution.

Currently, mechanistic FIB models range in complexity from simple mass balance equations (Boehm, 2003; Boehm et al., 2005; Kim et al., 2004) to 3D hydrodynamic simulations (Sanders et al., 2005; Liu et al., 2006; Thupaki et al., 2010; de Brauwere et al., 2011; Zhu et al., 2011). In conjunction with field observations and laboratory studies, these models have been used to identify processes structuring nearshore FIB contamination such as alongshore currents (Kim et al., 2004; Liu et al., 2006; Thupaki et al., 2010), tides (de Brauwere et al., 2011), internal waves (Wong et al., 2012), rip cells (Boehm, 2003; Boehm et al., 2005), cross-shore diffusion (Thupaki et al., 2010; Zhu et al., 2011), sediment resuspension (Sanders et al., 2005), solar insolation (Boehm et al., 2009; Liu et al., 2006; Thupaki et al., 2010), and temperature (de Brauwere et al., 2011). To date, however, only a handful of studies have used models to look at the relative importance of these processes in the nearshore. Thupaki et al. (2010) used a 3D hydrodynamic model to show that FIB loss in Lake Michigan due to alongshore current reversals and diffusion was over an order of magnitude greater than loss due to mortality. Zhu et al. (2011), however, revealed the opposite pattern in a quiescent Florida embayment. Furthermore, simple mass budget models for Califor-

---

* Corresponding author. Tel.: +1 831 419 5285.
E-mail address: mrippy@ucsd.edu (M.A. Rippy).

[1] Present address: P.O. Box 239, Kalaheo, HI 96741, USA.

0025-326X/$ - see front matter © 2012 Elsevier Ltd. All rights reserved.
http://dx.doi.org/10.1016/j.marpolbul.2012.09.030

nia's Huntington State Beach suggest that multiple processes can interchangeably dominate FIB dynamics (Boehm, 2003; Kim et al., 2004; Boehm et al., 2005; Grant et al., 2005). Taken together, these studies imply that the processes controlling surfzone FIB are likely to vary both in time (at a given beach), and space (beach to beach). Thus far, however, our analyses have been limited to the most nearshore of waters, as the majority of FIB data collected and used to calibrate models come from ankle- to knee-deep samples (Grant et al., 2001; Boehm, 2003; Liu et al., 2006; Thupaki et al., 2010). Recreational beach use, especially in California (where surfing is common), is not limited to the shoreline. This makes it important to evaluate FIB contamination and the processes controlling it over wider recreational domains where physical processes are different, and FIB survivorship may also change (Davies-Colley et al., 1994; Kim et al., 2004).

Here we present results from an along and cross-shore resolved field program with joint physical and bacterial observations designed to identify the dominant mechanisms controlling FIB variability within (and seaward) of the surfzone. By directly measuring currents out to 300 m cross-shore, we both enable the evaluation FIB flow fields over appropriate recreational domains, and avoid estimating current velocity from wave direction or alongshore drift, which has increased uncertainty in other models (Boehm, 2003; Kim et al., 2004). In the present paper we focus on quantifying the contribution of physical processes (advection and diffusion) to observed FIB patterns, and developing a best-fit physical model from this analysis. The contribution of biological processes to nearshore FIB variability is addressed in Rippy et al. (2012).

2. Methods

2.1. Field site description

Southern California's Huntington State Beach is ~3.2 km long, with chronically poor surfzone water quality (Grant et al., 2001; Kim et al., 2004). At its southern end, the beach receives brackish flows from the Talbert Marsh (TM) and the Santa Ana River (SAR), both of which have been implicated as sources of surfzone FIB (Kim et al., 2004). In fall 2006, a multi-institutional field campaign ("HB06") focused on observing nearshore waves, currents, temperature, phytoplankton, and FIB at this beach. The present study concerns the bacterial component of HB06, a 5-h FIB survey with high spatial and temporal resolution conducted on October 16th along transects extending 1 km north of the TM/SAR outlets, and 300 m offshore.

2.2. FIB sampling program

2.2.1. Sample collection and processing

FIB concentrations were measured at 8 stations: 4 in knee-deep water along a 1000 m alongshore transect north of SAR (SAR, TM, FHM, F1; Fig. 1), and 4 along a 300 m cross-shore transect starting at F1 (knee-deep water), and terminating at an offshore Orange County Sanitation District mooring (OM) in ~8 m mean water depth (F1, F3, F5, F7, OM; Fig. 1). Every 20 min, from 0650 h to 1150 h PDT, 100 ml water samples were taken at all stations. Samples were stored on ice and transported to the Orange County Sanitation District (OCSD) within 6 h of collection. All samples were analyzed for *Escherichia coli* (IDEXX Colilert) and *Enterococcus* (EPA method 1600) concentrations by OCSD personnel.

2.2.2. Spatial and temporal patterns in bacterial decay

Temporal rates of FIB loss were estimated for each station from regressions of log (FIB) versus time. We refer to these FIB loss rates as "decay", where decay includes removal/dilution due to advection and diffusion as well as biological mortality. In contrast, the term "mortality" will be used to denote the portion of decay that is due to FIB senescence alone, and is *not* caused by the measured physical processes.

At stations where FIB concentrations dropped below minimum sensitivity standards for our bacterial assays (<10 MPN/100 ml for *E. coli* or <2 CFU/100 ml for *Enterococcus*) prior to the end of the study period, decay rates were calculated using only data up until these standards were reached (SI Fig. 1). Decay rates were compared across sampling stations to look for spatial patterns in bacterial loss. Decay rates were also compared across FIB groups (*E. coli* vs. *Enterococcus*) to identify group-specific patterns. Statistical analyses were performed using MATLAB (Mathworks, Natick, MA).

2.2.3. Nearshore instrumentation

Pressure sensors and Acoustic Doppler velocimeters (ADV's) (Sontek, 2004), both sampling at 8 Hz, were placed in the nearshore to monitor the wave and current field during our study. All instruments were mounted on tripod frames fixed on the seafloor at seven locations (F1–F7) along the shoreward-most 150 m of the cross-shore transect shown in (Fig 1.). Cross-shore resolved estimates of the alongshore current field were determined using 20 min averaged alongshore water velocities from each ADV.

2.3. 2D individual based FIB model

The contribution of physical processes in structuring FIB concentrations during HB06 was quantified using a 2D (x = alongshore, y = cross-shore) individual-based advection–diffusion or "AD" model for FIB (informed by the model of Tanaka and Franks, 2008). Only alongshore advection, assumed to be uniform alongshore, was included in the model. Both cross-shore and alongshore diffusivities were also included. These were assumed to be equal at any point in space, and alongshore uniform. The cross-shore variation of diffusivity was modeled as:

$$\kappa_h = \kappa_0 + \frac{(\kappa_1 - \kappa_0)}{2}\left(1 - \tanh\left(\frac{(y - y_0)}{y_{scale}}\right)\right) \qquad (1)$$

Here κ_0 is the background (offshore) diffusivity, κ_1 is the elevated surfzone diffusivity (Reniers et al., 2009; Spydell et al., 2007), y_0 is the observed cross-shore midpoint of the transition between κ_0 and κ_1 (i.e., the offshore edge of the surfzone) and y_{scale} determines the cross-shore transition width. Representative values of κ_1 (0.5 $m^2\,s^{-1}$) and κ_0 0.05 $m^2\,s^{-1}$) were chosen based on incident wave height and alongshore current measurements (Clark et al., 2010; Spydell et al., 2009). The observed width of the surfzone (i.e., the region of breaking waves) was used to determine y_0. Significant wave height was maximum at F4 and low at F1 and F2, suggesting that the offshore edge of the surfzone was between F2 and F4 (Fig. 2a); thus y_0 = 50 m, near F3. To give a rapid cross-shore transition between surfzone (F2) and offshore (F4) diffusivity, y_{scale} was set to 5 m (SI Fig. 2). The AD model was only weakly sensitive to the parameterization of y_{scale}, κ_0 and κ_1, with sensitivity varying by station (SI Fig. 3). Cross-shore advection was not included in the model, as alongshore samples were taken from the same water depth each time (i.e., following the tidal excursion). Neglecting cross-shore advection (including rips, etc.) will generally lead to conservative estimates of the contribution of physical dilution to FIB decay.

2.3.1. Particle motions

In the AD model, FIB particles are advected alongshore by 20 min average currents (u), that vary in the cross-shore (y). FIB particles diffuse along- and cross-shore by horizontal diffusion (κ_h). For a particle starting at (x_t, y_t), its position at ($x_{t+\Delta t}$, $y_{t+\Delta t}$) is:

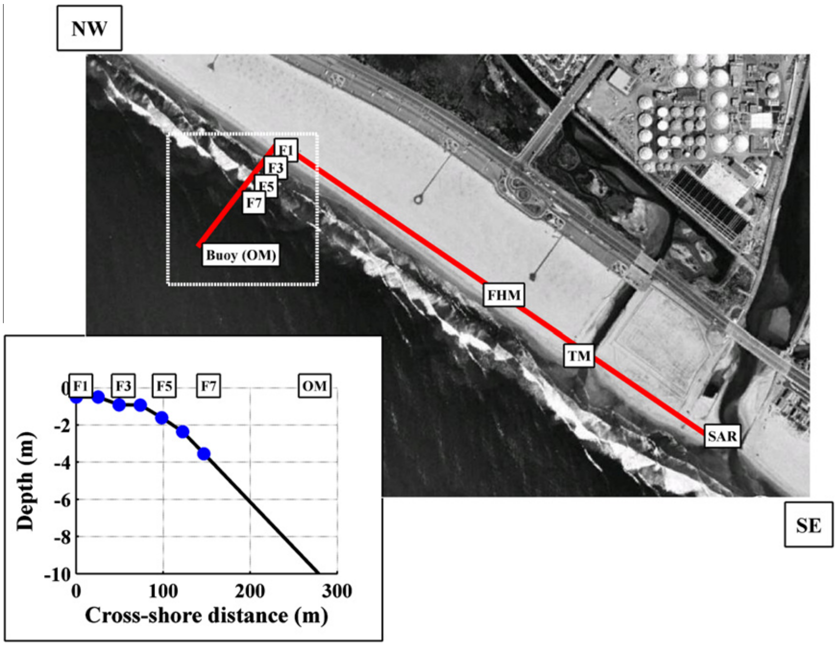

Fig. 1. Schematic of the HB06 experiment. White boxes mark the location of bacterial sampling stations. Alongshore sampling sites were the Santa Ana River (SAR), the Talbert Marsh (TM), a station 500 m north of the Santa Ana River (FHM), and the first surfzone frame (F1). Cross-shore sampling sites were located at the first (F1), third (F3), fifth (F5), and seventh (F7) surfzone frames as well as an offshore buoy (OM). Depth and distance offshore of cross-shore sites are shown in the inset, where blue circles mark the location of ADV's.

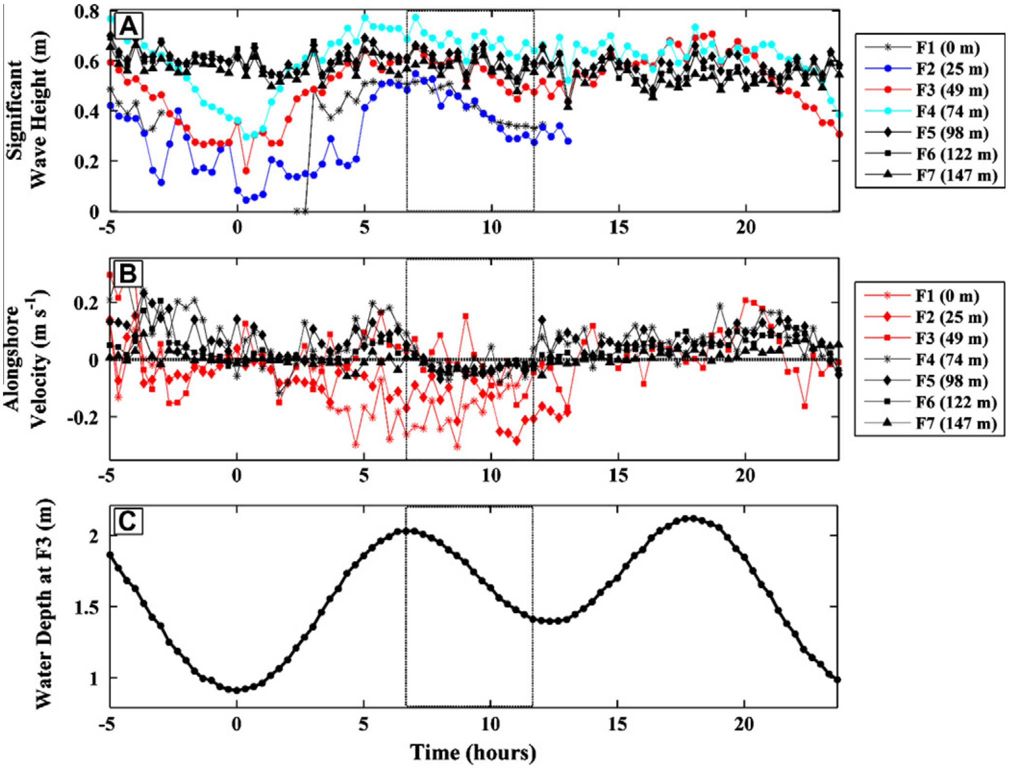

Fig. 2. (A) Significant wave height and (B) 20-min mean alongshore current (red = surfzone and black = offshore), measured at cross-shore frames F1–F7. (C) Mean water depth measured at F3 versus time (h) from 1950 on October 15th to 2350 on October 16th. Midnight is at $t = 0$ h. Dashed boxes indicate the 5-h HB06 FIB study period.

$$x_{t+\Delta t} = x_t + \frac{\partial \kappa_h(y_t)}{\partial y}\Delta t + R\sqrt{\frac{2\kappa_h}{r}\left(y_t + \frac{1}{2}\frac{\partial \kappa_h}{\partial y}\Delta t\right)\Delta t} + u\Delta t \qquad (2)$$

$$y_{t+\Delta t} = y_t + \frac{\partial \kappa_h(y_t)}{\partial y}\Delta t + R\sqrt{\frac{2\kappa_h}{r}\left(y_t + \frac{1}{2}\frac{\partial \kappa_h}{\partial y}\Delta t\right)\Delta t} \qquad (3)$$

where R is a random number with zero mean and variance r. For this model, $r = 1/3$, giving R a uniform distribution with range $[-1\,1]$ (Ross and Sharples, 2004; Tanaka and Franks, 2008). The time step was $\Delta t = 1$ s for all model runs. A reflecting boundary condition was used at the shoreline; otherwise particles could move anywhere in the domain.

2.3.2. Model initialization

The AD model was initialized at $t_0 = 0650$ h (the earliest FIB sampling time) with 80,000 bacterial particles distributed uniformly within a rectangular (x, y) patch. Each particle represents a number of FIB (concentration C); the actual number of FIB per particle can be scaled to match the data, provided the same scaling is applied to every particle. Our scaling constants were determined such that the space–time mean of AD modeled FIB equaled the space–time mean of measured FIB (*E. coli* or *Enterococcus*).

Initial patch boundaries (along and cross-shore) were identified by varying patch boundary locations over reasonable ranges to maximize the skill between the AD model and HB06 FIB data. Skill is defined as:

$$\text{Skill} = 1 - \frac{\text{mean}(C_{obs} - C_{mod})^2}{\text{mean}(C_{obs} - \overline{C}_{obs})^2} \tag{4}$$

where C_{obs} are log FIB concentration data, C_{mod} are log AD model outputs, and $\overline{C}_{obs}$ is the space–time mean of $\log(C_{obs})$ for all stations and times (Krause et al., 2005). Here, skill is a measure of how much better (or worse) the model explains fluctuations in the data than the data mean. A value of 0 indicates that the model performs the same as the data mean. A value of 1 indicates that the model explains all the variance after removing the mean, and a negative value indicates that the model performs worse than the data mean. Depending on the context, the numerator for skill was calculated for individual stations, groups of stations, or all stations together; the denominator was always the same (all stations).

HB06 FIB observations showed the offshore FIB patch edge to be ~140–300 m from the shoreline. The effect of this range of possible offshore patch edges was explored in the model. The northernmost patch edge was varied from 0 to 2000 m north of the sampling region, and the southernmost patch edge was varied from 0 to 2000 m south of the sampling region. The initial patch always included the 1 km-long sampling region. Initial patch sizes that maximized alongshore and cross-shore station skill were used to initialize a "best-fit" AD model for subsequent comparisons between modeled and observed FIB concentrations and decay rates. The robustness of the model to alternative initial patch shapes is discussed briefly below (for details see SI methods and SI Fig. 4).

3. Results and discussion

3.1. Physical environment

On October, 16th, 2006, the surfzone was between 40 and 70 m wide, with wave breaking beginning between F2 and F4. The maximum significant wave height was about 0.8 m, at F4 (Fig. 2a). The alongshore current direction (u) was variable both in time and with distance across shore. During the 5 h of FIB sampling, inner surfzone u (F1 and F2) was typically southward, while outer surfzone u (F3) and offshore u (F4–F7) were initially northward, and then reversed between 0750 h and 0930 h (Fig. 2b). The reason for the current reversal at F3 and farther offshore is unknown, but may be linked to tidal phase, which transitioned from flood to ebb at 0710 h (Fig. 2c).

The cross-shore sign reversal of the alongshore currents during the first hour of FIB sampling was also observed in the 12 h prior to FIB sampling (Fig. 2b). During this time, the average surfzone current was flowing south (0.03 m s^{-1}), and the average offshore current was flowing north (0.05 m s^{-1}) (Fig. 2b), suggesting that offshore and surfzone FIB could have originated from different alongshore sources separated by as much as 5 km.

To identify possible source locations for the bacterial pollution observed on October 16th in more detail, the advection–diffusion (AD) model (described above) was initialized with a uniform rectangular patch of particles spanning the study region (150 m cross-shore by 1000 m alongshore). The model was then run backwards in time (hindcast) to sundown of the previous evening using measured alongshore currents and no diffusion. These analyses showed that the surfzone FIB may have originated from a source 600–1500 m north of the study area, whereas the offshore FIB probably originated from a southern source, anywhere from 2 to 5 km south of the study area (Fig. 3).

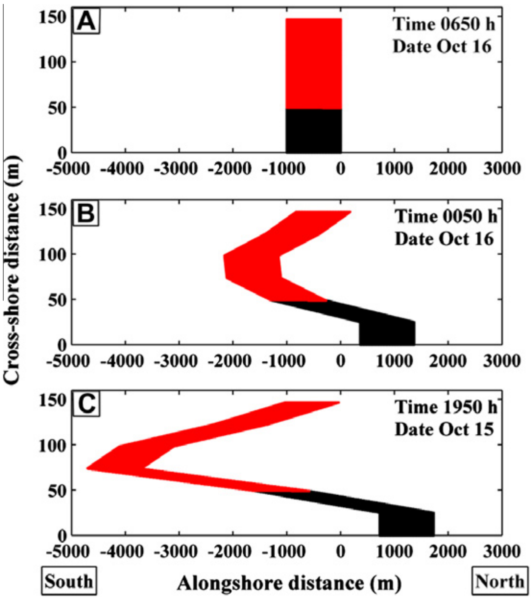

Fig. 3. Along- and cross-shore locations of FIB particles initialized in a uniform rectangular patch at 0650 (A) and advected back in time using measured alongshore currents for six (B), and 11 (C) h. Surfzone FIB particles are black and offshore FIB particles are red. Particle locations reflect cross-shore shear in the alongshore current, with surfzone FIB originating to the north and offshore FIB originating to the south. The origins of surfzone FIB appear stable around 600–1500 m N, while the origins of offshore FIB are time dependent (B and C).

3.2. Bacterial patterns at Huntington Beach

At 0650 h on October 16th, *E. coli* and *Enterococcus* concentrations exceeded EPA single-sample standards (104 *Enterococcus*/100 ml and 235 *E. coli*/100 ml) at most stations (88% for *E. coli* and 75% for *Enterococcus*). FIB concentrations were near zero offshore at OM, and concentrations at TM were approximately half those of the other stations (Fig. 4). The low concentrations at OM are consistent with prior research suggesting shoreline sources of FIB at Huntington Beach (Grant et al., 2001; Kim et al., 2004), and the retentive nature of the surfzone (Clark et al., 2010; Grant et al., 2005; Spydell et al., 2009). The low concentrations at TM, however, were unexpected, as prior research at Huntington Beach has shown a connection between *Enterococcus* concentrations and bird feces in the marsh (Grant et al., 2001; Kim et al., 2004).

By 1150 h, FIB concentrations at all sampling locations were well below morning levels (Fig. 4). FIB decay was exponential in time at all stations, with *Enterococcus* concentrations decaying significantly faster than *E. coli* concentrations (Table 1).

3.3. Spatial structure of FIB decay

E. coli and *Enterococcus* decay rates varied spatially, and were faster to the north than the south. FIB decay rates were not always significantly different at adjacent alongshore stations, but decay at SAR (southernmost station) was always slower than at F1 (northernmost station; Fig. 5a). There were no significant differences in

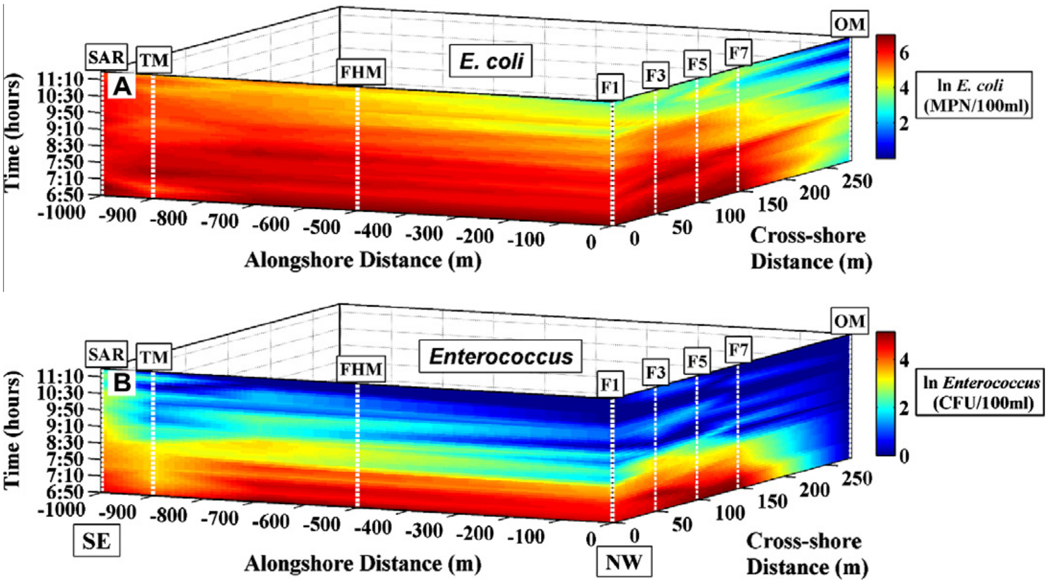

Fig. 4. Contour plots of (A) *E. coli* (ln MPN 100 ml^{-1}), and (B) *Enterococcus* (ln CFU 100 ml^{-1}) concentrations at HB06 as a function of cross-shore distance (m), alongshore distance (m), and time (h). Plots are oriented as though the viewer is standing on the beach, looking offshore. On the alongshore axis, the northernmost station is located at 0 m, with negative values indicating stations to the south. The location of each sampling station is shown by a dashed white line.

Table 1
Rates of FIB decay during HB06.

Station	*E. coli* decay[a] (MPN s^{-1}) $\times 10^{-4}$	*E. coli* R^2	*Enterococcus* decay[a] (CFU s^{-1}) $\times 10^{-4}$	*Enterococcus* R^2	*E. coli vs Ent.* decay ANCOVA F-stat
SAR	−0.37	0.48[*]	−1.40	0.91[**]	41.66[**]
TM	−0.69	0.50[*]	−1.96	0.85[**]	21.61[**]
FHM	−0.11	0.80[**]	−2.41	0.91[**]	36.06[**]
F1	−2.04	0.89[**]	−3.85	0.89[**]	19.59[**]
F3	−2.08	0.89[**]	−3.32	0.81[*]	12.70[*]
F5	−2.16	0.89[**]	−3.71	0.91[**]	19.64[**]
F7	−2.29	0.87[**]	−4.41	0.89[**]	18.90[**]
OM	−1.24	0.18	0.00	0.00	–

[*] Significance at $p < 0.01$.
[**] Significance at $p < 0.001$.
[a] FIB decay rates (and R^2 estimates) were calculated from exponential regressions of logged FIB data vs time.

FIB decay rates across shore for either FIB group (Fig. 5b). The similar along- and across shore spatial patterns in decay observed for *E. coli* and *Enterococcus* suggest that, although the magnitude of decay may vary with FIB group (mentioned above), both groups are affected by similar overarching processes such as physical dilution by advection and diffusion. We will quantify the contribution of advection and diffusion to measured FIB decay using our AD model.

3.4. Model sensitivity analysis: initial patch size

Due to predominately southward advection during the sampling period, the AD model was sensitive to initial (0650 h) offshore and northern patch boundaries, but not the southern boundary. We modified Eq. (4) to calculate skill at alongshore or cross-shore stations only, as we varied the northern and offshore edges of the initial patch, respectively. Alongshore skill was maximum when the initial northern patch edge was 200 m N of F1 for *Enterococcus* and 600 m north of F1 for *E. coli* (Skill = 0.60 and 0.85, respectively) (SI Fig. 5a). Notably, however, alongshore skill was relatively constant for initial northern patch edges between 100 and 900 m north (*E. coli*) or 100 and 600 m north (*Enterococcus*) (SI Fig. 5a). For subsequent AD model runs, the northern patch edge was set to 600 m north; this value lies within the region of high model skill for *E. coli* and *Enterococcus* (SI Fig. 5a). It is also consistent with the results of our hindcast model (Fig. 3), which indicated that surfzone FIB originated 600–1500 m north of the study area.

Overall, cross-shore AD model skill was lower than alongshore skill. Maximum cross-shore skill occurred when the initial offshore patch edge was 160 m offshore for both FIB groups (Skill = 0.16 and 0.29, respectively) (SI Fig. 5b).

The optimal northern and offshore initial patch boundaries identified in this manner (600 m north and 160 m offshore) were relatively robust to initial patch shape. Initializing the model with a rectangular patch that had diffused for 5 h, instead of a rectangular patch with sharp edges, identified similar patch boundaries (700 m north and 160 m offshore) with reduced model skill, especially in the cross-shore (SI Figs. 4 and 5).

3.5. Best-fit model-data comparisons: physical factors controlling FIB patchiness

The AD (advection and diffusion) model reproduced a statistically significant amount of FIB variability at alongshore stations during HB06. Modeled FIB concentrations decayed markedly (especially at northern stations) by 1150 h, as was observed in the field (Figs. 4 and 6a). Station-specific model skill was typically high (Skill = 0.74–0.90 for *E. coli*, and 0.45–0.66 for *Enterococcus*), with lower skill observed for *Enterococcus* (Fig. 6b). Modeled station-specific FIB decay – driven only by advection and diffusion – was exponential for all alongshore stations (SI Fig. 6), and exhibited a spatial pattern similar to HB06 FIB data, with significantly faster decay observed at northern stations than southern stations (Fig. 5a). Although the spatial patterns of decay estimated by the AD model matched those of HB06 FIB well, the actual magnitudes of the decay rates were lower than observed (Fig. 5). The only station where the AD model captured FIB decay rates accurately ($p < 0.05$) was SAR, for *E. coli* (Fig. 5a). At all other stations, AD modeled FIB decay accounted for ⩽50% of observed decay (Fig. 5). This underestimation of FIB decay rates suggests that an

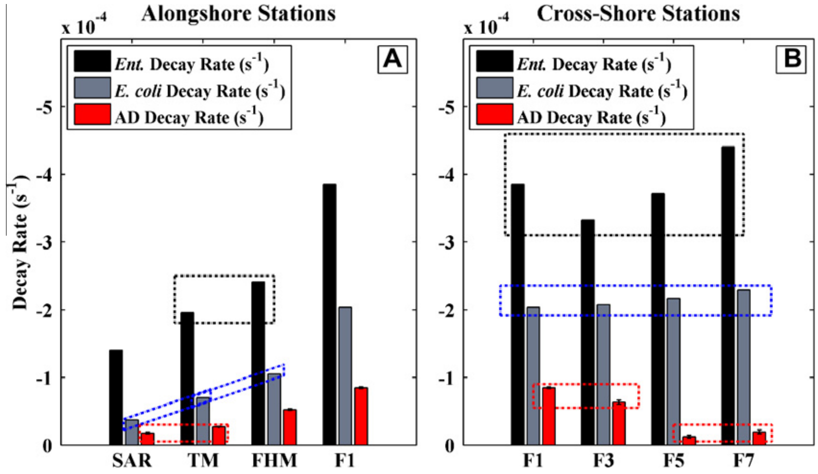

Fig. 5. Bar graph of measured exponential decay rates for *Enterococcus* (black bars) and *E. coli* (gray bars), and FIB modeled using the AD model (red bars). (A) Alongshore sampling stations and (B) cross-shore sampling stations. FIB decay rates from the AD model are averages of 10 model runs, shown with standard error. Boxes link stations for *Enterococcus* (black), *E. coli* (blue) and the AD model (red) with decay rates that are not significantly different from one another ($p < 0.05$). See SI Fig. 1 for exponential fits to FIB data.

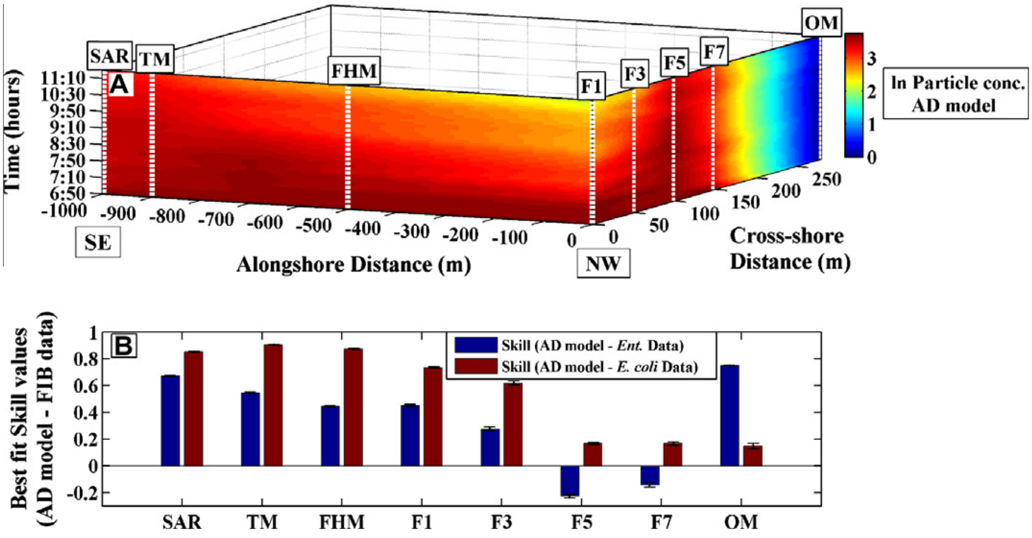

Fig. 6. (A) Contour plot of best-fit AD model particle concentrations as a function of cross-shore distance (m), alongshore distance (m), and time (h). Axes are same as Fig. 4. (B) Bar graph of station-specific skill for AD model – FIB data comparisons; *Enterococcus* (blue) and *E. coli* (red).

additional source of decay must be included in the model to accurately reproduce FIB dynamics during HB06. This additional decay is likely to be intrinsic to the FIB taxa, as the amount of unexplained FIB decay during HB06 was group-specific (Fig. 5).

In the cross-shore, the AD model successfully reproduced FIB patterns for surfzone stations (F1, F3) and the offshore mooring (*Enterococcus* only), where FIB concentrations were consistently near zero. It failed, however, to reproduce FIB patterns for offshore stations exhibiting FIB contamination (F5, F7) (Fig. 6b). Poor model-data fits at these stations likely reflect over-retention of offshore FIB (Figs. 4 and 6a). Modeled FIB decay at these stations was significantly slower than decay at F1 and F3, while observed FIB decay rates were constant across-shore (Fig. 5b). Together, the relatively poor model-data fits and decay-rate estimates for offshore stations suggest that, although the AD model performs well in the surfzone, it is missing a dominant process structuring offshore FIB concentrations during HB06.

Through a synthesis of field observations and models, we have shown that a model including only horizontal advection and diffusion can explain a significant portion of the variability in FIB concentrations at Huntington Beach, especially in the alongshore (Skill of 0.45–0.90 at alongshore stations and −0.23 to 0.74 at cross-shore stations, Fig. 6b). To our knowledge, HB06 is the first study to perform high-resolution monitoring of FIB, waves, and currents both in the surfzone and offshore, providing an opportunity to directly quantify the importance of these physical processes in structuring nearshore FIB pollution. The strong role of advection and diffusion in structuring patterns of FIB during HB06 was somewhat surprising given the temporal decays observed at each sampling station often attributed to solar insolation (e.g., Ki et al., 2007). Our analyses suggest, however, that a significant portion of this decay (mean of 38% for *E. coli*, and 14% for *Enterococcus*) was due to southward advection and diffusion of FIB patches through the study area (Fig. 5). This resulted in faster FIB decay to the north than the south, as the FIB patch was mixed and advected past northern stations first.

Note that the contribution of physical processes to FIB dynamics reported here is specific to our study date on October 16th. Because our AD model was not validated with an independent data set, it is not suitable for forecasting or prediction. The model, however, does provide a baseline for estimating the degree of control advection and diffusion are likely to have on FIB at Huntington Beach, as the contribution of these processes to FIB dynamics should increase/decrease as a function of the magnitude of nearshore mixing/transport.

Although the AD model captured FIB dynamics during HB06 well overall, the underestimation of FIB decay rates (especially at offshore stations) suggests that it is missing important processes governing FIB decay. Given the reported sensitivity of FIB to variations in solar insolation, organic matter, pH, salinity, etc., it is likely that some form of extra-enteric FIB mortality may have contributed to the FIB decay observed during HB06 (Anderson et al., 2005; Curtis et al., 1992; Sinton et al., 2002). The contribution of mortality to nearshore FIB variability is addressed in Rippy et al. (2012).

Acknowledgements

This work was partially funded by NSF, ONR, CA SeaGrant (NOAA project #NA10OAR4170060, California Sea Grant Project #25793B; through NOAA's National Sea Grant College Program, U.S. Dept. of Commerce), the California Coastal Conservancy, the California Department of Boating and Waterways Oceanography Program, and NOAA. The statements, findings, conclusions and recommendations are those of the author(s) and do not necessarily reflect the views of the aforementioned organizations. Tests for FIB analysis were provided and performed by the Orange County Sanitation District. Special thanks to volunteers and staff from the Integrative Oceanography Division (B. Woodward, B. Boyd, D. Clark, K. Smith, D. Darnell, I. Nagy, J. Leichter, M. Omand, M. Okihiro, M. Yates, M. McKenna, S. Henderson, D. Michrokowski) for their assistance in data collection.

Appendix A. Supplementary material

Supplementary data associated with this article can be found, in the online version, at http://dx.doi.org/10.1016/j.marpolbul.2012.09.030.

References

Anderson, K.L., Whitlock, J.E., Harwood, V.J., 2005. Persistence and differential survival of fecal indicator bacteria in subtropical waters and sediments. Appl. Environ. Microbiol. 71, 3041–3048.

Boehm, A.B., 2003. Model of microbial transport and inactivation in the surfzone and application to field measurements of total coliform in northern Orange County California. Environ. Sci. Technol. 37, 5511–5517.

Boehm, A.B., Grant, S.B., Kim, J.H., Mowbray, S.L., McGee, C.D., Clark, C.D., Foley, D.M., Wellman, D.E., 2002. Decadal and shorter period variability of surfzone water quality at Huntington Beach. California Environ. Sci. Technol. 36, 3885–3892.

Boehm, A.B., Keymer, D.P., Shellenbarger, G.G., 2005. An analytical model of enterococci inactivation, grazing, and transport in the surfzone of a marine beach. Water Res. 39, 3565–3578.

Boehm, A.B., Yamahara, K., Love, D.C., Peterson, B.M., McNeill, K., Nelson, K.L., 2009. Covariation and photoinactivation of traditional and novel indicator organisms and human viruses at a sewage impacted marine beach. Environ. Sci. Technol. 43, 8046–8052.

Clark, D.B., Feddersen, F., Guza, R.T., 2010. Cross shore surfzone tracer dispersion in an alongshore current. J. Geophys. Res. 115, C10035–C10053.

Curtis, T.P., Mara, D.D., Silva, S., 1992. Influence of pH, oxygen, and humic substances on ability of sunlight to damage fecal coliforms in waste stabilization pond water. Appl. Environ. Microbiol. 58, 1335–1343.

Davies-Colley, R.J., Bell, R.G., Donnison, A.M., 1994. Sunlight inactivation of enterococci and fecal coliforms in sewage effluent diluted in seawater. Appl. Environ. Microbiol. 60, 2049–2058.

de Brauwere, A., de Brye, B., Servais, P., Passerat, J., Deleersnijder, E., 2011. Modeling *Escherichia coli* concentrations in the tidal Scheldt river and estuary. Water Res. 45, 2724–2738.

Dufour, A.P., Wymer, L.J., 2006. Microbes, monitoring, and human health. Oceanography 19, 72–80.

Grant, S.B., Sanders, B.F., Boehm, A.B., Redman, J.A., Kim, J.H., Mrse, R.D., Chu, A.K., Gouldin, M., McGee, C.D., Gardiner, N.A., Jones, B.H., Svejkovsky, J., Leipzig, G.V., Brown, A., 2001. Generation of enterococci bacteria in a coastal saltwater marsh and its impact on surfzone water quality. Environ. Sci. Technol. 35, 2407–2414.

Grant, S.B., Kim, J.H., Jones, B.H., Jenkins, S.A., Wasyl, J., Cudaback, C., 2005. Surfzone entrainment, along-shore transport, and human health implications of pollution from tidal outlets. J. Geophys. Res. 110, C10025–C10045.

Ki, J., Ensari, S., Kim, H.J., 2007. Solar and tidal modulations of fecal indicator bacteria in coastal waters at Huntington Beach California. Environ. Manage. 39, 867–875.

Kim, J.H., Grant, S.B., 2004. Public mis-notification of coastal water quality: a probabilistic evaluation of posting errors at Huntington Beach. Environ. Sci. Technol. 8, 2479–2504.

Kim, J.H., Grant, S.B., McGee, C.D., Sanders, B.F., Largier, J.L., 2004. Locating sources of surfzone pollution: a mass budget analysis of fecal indicator bacteria at Huntington Beach California. Environ. Sci. Technol. 38, 2626–2636.

Krause, P., Boyle, D.P., Base, F., 2005. Comparison of different efficiency criteria for hydrological model assessment. Adv. Geosci. 5, 89–97.

Liu, L., Phanikumar, M.S., Molloy, S.L., Whitman, R.L., Shively, D.A., Nevers, M.B., Schwab, D.J., Rose, J.B., 2006. Modeling the transport and inactivation of *E. coli* and enterococci in the near-shore region of lake Michigan. Environ. Sci. Technol. 40, 5022–5028.

Reniers, A.J.H.M., MacMahan, J.H., Thornton, E.B., Stanton, T.P., Henriquez, M., Brown, J.W., Brown, J.A., Gallagher, E., 2009. Surfzone surface retention on a rip-channeled beach. J. Geophys. Res. 114, C10010–C10022.

Rippy, M.A., Franks, P.J.S., Feddersen, F., Guza, R.T., Moore, D.F., 2012. Factors controlling variability in nearshore fecal pollution: The effects of mortality. Mar. Pollut. Bull., in press. http://dx.doi.org/10.1016/j.marpolbul.2012.09.003.

Ross, O.N., Sharples, J., 2004. Recipe for 1-D Lagrangian particle tracking models in space-varying diffusivity. Limnol. Oceanogr. Methods 2, 289–302.

Sanders, B.F., Arega, F., Sutula, M., 2005. Modeling the dry-weather tidal cycling of fecal indicator bacteria in surface waters of an intertidal wetland. Water Res. 39, 3394–3408.

Sinton, L.W., Donnison, A.M., Hastie, C.M., 1993. Faecal streptococci as faecal pollution indicators: a review. Part 1: Taxonomy and enumeration. New Zealand J. Marine Freshwater Res. 27, 101–115.

Sinton, L.W., Hall, C.H., Lynch, P.A., Davies-Colley, R.J., 2002. Sunlight inactivation of fecal indicator bacteria and bacteriophages from waste stabilization pond effluent in fresh and saline waters. Appl. Environ. Microbiol. 68, 1122–1131.

Sontek, 2004. Sontek ADV Field Accoustic Doppler Velocimeter: Technical Documentation. Sontek/YSI, San Diego.

Spydell, M., Feddersen, F., Guza, R.T., Schmidt, W.E., 2007. Observing surf-zone dispersion with drifters. J. Phys. Oceanogr. 37, 2920–2939.

Spydell, M.S., Feddersen, F., Guza, R.T., 2009. Observations of drifter dispersion in the surfzone: the effect of sheared alongshore currents. J. Geophys. Res. 114, C07028–C07045.

Tanaka, Y., Franks, P.J.S., 2008. Vertical distributions of Japanese sardine (*Sardinops melanosticus*) eggs: a comparison of observations and a wind-forced Lagrangian mixing model. Fish. Oceanogr. 17, 89–100.

Thupaki, P., Phannikumar, M.S., Beletsky, D., Schwab, D.J., Nevers, M.B., Whitman, R.L., 2010. Budget analysis of *Escherichia coli* at a southern Lake Michigan beach. Environ. Sci. Technol. 44, 1010–1016.

Wong, S.H.C., Santoro, A.E., Nidzieko, N.J., Hench, J.L., Boehm, A.B., 2012. Coupled physical, chemical, and microbiological measurements suggest a connection between internal waves and surfzone water quality in the Southern California Bight. Cont. Shelf Res. 34, 64–78.

Zhu, X., Wang, J.D., Solo-Gabriele, H.M., Fleming, L.E., 2011. A water quality modeling study of non-point sources at recreational marine beaches. Water Res. 45, 2985–2995.